Increasing Sequential Tropical Cyclone Hazards from Historical to Future Climates in the U.S. East and Gulf Coasts

Dazhi Xi
Princeton University https://orcid.org/0000-0002-4096-8441
Ning Lin (nlin@princeton.edu)
Princeton University https://orcid.org/0000-0002-5571-1606
Avantika Gori
Princeton University

Article

Keywords:

Posted Date: June 29th, 2022

DOI: https://doi.org/10.21203/rs.3.rs-1744996/v1

Version of Record: A version of this preprint was published at Nature Climate Change on February 27th, 2023. See the published version at https://doi.org/10.1038/s41558-023-01595-7.

Abstract

Sequential landfalling tropical cyclones (TCs) pose great risks to coastal areas. Here we find that the chance of two hazard-producing TCs occurring within 15 days has been increasing at some U.S. locations (e.g., the probability doubled over the past 7 decades for Sandy Hook, NJ). We show that under the high emission scenario SSP5 8.5, the return period of two hazard-producing TCs impacting the same location within 15 days may decrease over the century by 80%-94% along the U.S. East and Gulf Coasts, due mainly to sea-level rise and rainfall intensification. Climate change can also cause unprecedented spatial compounding of extreme hazards. A Katrina-like TC and a Harvey-like TC impacting the U.S, within 15 days, which is non-existent in the control simulation for over a thousand years, is projected to have an annual occurrence probability greater than 1% by the end of the century under the high emission scenario.

Introduction

Compound extreme weather events are hazardous and can produce higher impacts than individual events combined. Compound events may be classified into multivariate events, spatially compounding events, and temporally compounding events [1]. Multivariate events refer to the events in which multiple hazards occur at the same time while spatially compounding events occur when multiple locations in a region are impacted by the hazards within a limited time window[1]. Temporally compounding events refer to multiple hazardous events happening consecutively, and the later hazards can produce more damage due to the lowered resistance of infrastructure and communities caused by the earlier events. For example, TCs and heatwaves can be temporally compounded. A TC may destroy the power system, leaving residents without air conditioning when a following heatwave arrives[2,3].

TCs themselves can generate multiple hazards: strong winds, rainfall, and storm surges. These hazards can weaken coastal infrastructure[4], leaving coastal communities vulnerable for weeks or months. These hazards can happen jointly (e.g., compound flooding [5,6]) and produce significant damage. However, previous studies have focused only on the joint hazards from pairs of TC hazards[5–8]. A study of the triple TC hazards (i.e., wind, surge, and rainfall) is needed to gain comprehensive understanding of TC hazards. Furthermore, previous study has not addressed sequential hazards from TCs, which have recently made significant impacts in the United States. For example, Fig. 1 shows the hazards caused by Hurricane Ida (2021) and Hurricane Nicholas (2021) in Louisiana; the interval between the hazards from the two storms is less than 15 days[8]. Investigations found that the influence of the earlier storm, Ida, (e.g., flooding roads) led to a more significant impact by the later storm, Nicholas [9,10]. The recent occurrence of such sequential hazard events appears to be consistent with previous findings that the chance of TCs making sequential landfall is increasing[11] and TCs are becoming more capable of producing hazards[6,12,13]. However, it is still unclear whether the occurrence rate of sequential TC hazards in the historical period shows any trends, if we can make robust projections of such events considering the uncertainties in TC

frequency projection[14], and which leading physical mechanisms cause the change (if any) of sequential TC hazards.

To address these questions, we investigate the change of sequential TC hazards using both historical observations and climate simulations. We choose the yearly minimal impact interval (MII) between hazard-producing TCs at a location as a metric for the analysis of sequential TC hazards. We define thresholds for individual hazard components (surge, rain, and wind) as the 95-th percentile of TC daily maximum water level, daily total rainfall, and daily maximum wind, respectively, and define the storms with at least one hazard component exceeding the threshold to be hazard-producing TCs. The MII is then the yearly minimal of the intervals between the durations of hazards (above the thresholds) of two consecutive TCs (sensitivity tests of the hazard definition performed by using other percentiles; see Methods). We focus on the sequential impact from storm hazards at the same location (temporally compounding events). We also present a brief analysis of the sequential impact from severe TCs (such as Harvey and Katrina) along the U.S. coastline (spatially compounding extremes). As an additional reference, we analyze marginal and joint TC wind, surge, and rainfall hazards (multivariate events), to also help us understand the causation of changes in sequential TC hazards.

Detecting the historical trend of sequential TC hazards directly from observations is challenging due to data limitations[11]. To circumvent the challenge, we expand a probabilistic model[11] that describes the landfall of sequential TCs (see Methods) and fit the model using historical observations of sequential TC hazard events. The model is then used to perform Monte Carlo simulations for each year from 1949 to 2018 to generate a large sample of sequential TC hazard events for 9 selected locations along the U.S. East and Gulf coasts, to estimate the historical trend of sequential TC hazards (Methods).

For future projection, we apply a physics-based TC hazard analysis method to investigate sequential TC hazards impacting the U.S. Gulf and East Coasts under the combined influence of SSP5 8.5 TC climatology and RCP 8.5 sea-level rise (SLR) [6]. We use the synthetic TCs generated from a statistical-deterministic TC model[6,15] forced by 6 Coupled Model Intercomparison Project Phase 6 (CMIP6) climate models (CanESM5, CNRM-CM6-1, GFDL-CM-4, EC-Earth3, IPSL-CM6A-LR, MIROC6). For each storm, we simulate storm tides with the advanced circulation (ADCIRC) hydrodynamic model[16], rainfall with the physics-based TC rainfall (TCR) model[17,18], and wind using a complete wind profile (C15) model[19]. To evaluate the impact of SLR on sequential TC hazard events, we incorporate the spatially varied, probabilistic SLR projection[20]. The abovementioned probabilistic model of sequential TC hazards is then fitted by the simulated TC hazards to investigate the change of the return periods of MII from the historical to future climates (Methods). To better understand the physical drivers of the change of sequential hazards, the changes of the TC single and joint hazards are also explored through investigating the probability of hazard components individually or jointly exceeding the historical return levels in the future climate (Methods).

Results

Increased Probability of Hazard-Producing Storms from 1949–2018

The scarcity of sequential TC hazard events in observation prevents direct detection of any trend. For example, for the 9 U.S. locations along the Gulf and Atlantic coasts analyzed in this study (shown in Supplementary Fig S1), the most frequent sequential TC hazard events (e.g., MII < 20day) are found in Wilmington (NC), which happened twice during 1949–2018. However, several parameters that control the occurrence of sequential hazard-producing storms can be analyzed based on historical events. These parameters include annual frequency of TC hazard and hazard durations. We analyze the trends in hazard frequency and hazard duration (exceeding the 95th percentile) for the 9 coastal locations. Except for Charleston, SC, the hazard frequency has increased since 1949 (Fig S2), mainly caused by the increase of TC's hazard-producing capability (Fig S3) rather than landfall frequency (Fig S4). The increase of TCs' hazard-producing ability is likely a result of the increased TC intensity[21]. Except for Charleston, SC, the hazard duration has also increased since 1949 (Fig S5), which may be a result of decreased TC translation speed[22] and prolonged stalling times[23] near the coastline.

For most selected locations, the change of frequency and duration of hazard-producing storms both favor an increased trend of sequential TC hazards. Figure 2 shows the yearly probability of experiencing sequential hazard-producing TCs, which was estimated by the probabilistic model with the hazard frequency and duration parameters fitted for each year (10-year moving-average). Except for Charleston, SC, there is a clear increasing trend of the probability of sequential hazard-producing storms. For example, the probability doubled over the past 7 decades for Sandy Hook, NJ. At all locations except Fort Pulaski, GA, the trend is largely driven by the higher probability in the decades from 1990–2010. The highest annual probability across the 9 locations in the past 7 decades of experiencing sequential hazard-producing TC events (MII < 30 days) is less than 10% (Charleston, SC in the 1980s), implying the rareness of such events and explaining why no trend can be detected directly.

Projected Increase of Sequential TC Hazards over the 21st Century

Climate projection based on the ensemble average of six climate models shows that the return period of MII of hazard-producing TCs will significantly decrease in all regions along the U.S. East and Gulf coasts by the end of the 21st century (Figure 3). The decrease is more dramatic if SLR is taken into consideration. For example, MII between the hazards from two sequential TCs smaller than 15 days is a 40-year event in the control climate for Texas, but in the future if we adapt to SLR, such an event will become a 10-year event; if we do not, it will become a 5-year event.

The estimated change of MII can be compared with the change of MII if the definition of "impact" is that the TC occurs within 250 km of the coastline (landfall) as considered by ref[11]. For example, for the 15-day MII return level, the decrease of return period defined by landfall ranges from -33% to -50% across U.S. East and Gulf coasts, while the decrease defined by hazard ranges from -80% to -94% considering SLR and -60% to -76% not considering it (Table S1). The decrease in the MII return period defined by

landfall is mainly a result of projected increase of landfalling TC frequency as shown in ref[11], while the increase of hazard-producing TC frequency is due to both increased landfall frequency and storm hazard-producing ability. The larger increase in sequential TC hazard events when considering SLR shows the significant influence of SLR on the occurrence of sequential hazard-producing TCs.

A major driver for shortened MII is the projected increase of landfall frequencies, which has large uncertainties[14]. However, a sensitivity test using future storms with the control frequency shows that the return period of MII will still decrease significantly, especially when SLR is considered. For example, in Texas, an MII of less than 15 days would change from a 40-year event to a 25-year event if we adapt to SLR and a 9-year event if we do not. The sensitivity test implies that the enhanced hazard severity[12,13] caused mainly by increased TC intensity[24–26], together with SLR, significantly increases the frequency of sequential hazards from TCs regardless of the uncertainty in TC frequency projection. The analysis results show that the change in MII return period solely due to increased hazard severity is comparable to the change in MII return period caused by increased landfall frequencies (Table S1).

Leading Mechanisms for the Increase of Future Sequential TC Hazards

The chance of sequential hazard-producing events was shown to significantly increase in the future due to the increased severity of TC hazards (Figure 3). Individual and joint TC hazards may become more severe and last longer. From the control (1984-2005) to the future climate (2070-2100), the return period of joint hazards (i.e., wind, surge, and rainfall jointly exceeding their historical return levels) will significantly decrease for all U.S. coastal regions (Fig. S12). Unrelated to storm frequency changes, the proportion of landfalling storms that can produce joint hazards (Figure 4) will increase from 3.16%-11.4% to 7.01%-26.38% (14.61%-30.63% with SLR). More directly related to the increase in sequential hazard events, the return period of hazard-producing events (i.e., at-least-one hazard exceeding the historical return level) will also significantly decrease across the United States (Fig. S13). The proportion of landfalling storms being hazard-producing will increase from 25.72%-41.95% to 34.52%-55.06% (78.93%-83.90% with SLR) (Figure 4).

To understand which hazard component of TCs (i.e., surge, rain, or wind) drives the change of the sequential events, the ratio between single hazard-producing TC frequency and landfall TC frequency was examined (Figure 4). In the control simulation, surge has the highest hazard-to-landfall ratio among the three hazards (ranging from 16.92%-37.21%). In the future climate simulation, if SLR is not taken into consideration (or the coastal areas are well adapted to the projected SLR), the leading hazard component switches to rainfall. For example, in Texas, the ratios in the control climate are 28.95%, 26.89%, and 25.48% and in the future climate 35.20%, 47.83%, and 38.07% for surge, rain, and wind hazard, respectively. The relative increase of the rate of rainfall hazard-producing TCs ranges from 69.3% to 120.6% across the coastal regions (Table S2). The increase of rainfall hazard is a result of the combination of TC climatology change and the increase of atmospheric water vapor content[27,28] , which may lead to a more significant increase of rainfall hazard than of other hazards.

If coastal communities do not adapt to the projected SLR, coastal extreme water level will be the leading hazard, and the ratio between surge hazard-producing storms to landfalling storm will reach 77.86%-82.95% (Figure 4). The relative increase of the rate of surge hazard-producing TCs ranges from 123.4% to 385.1%, and the relative increase of the rate of hazard-producing TCs ranges from 92.7% to 205.6% (Table S2). However, the increase of joint-hazard-producing TCs is not as significant as the increase of surge hazard-producing TCs. For example, in Texas, the relative increase of the rate of joint hazard TCs from not considering SLR to considering SLR is 31.1%; the relative increase for surge hazard TCs is 134.7%. This difference occurs because under SLR, weak TCs become capable of producing significant extreme water levels, but these TCs are not intense enough to produce extreme rainfall and wind. In addition to the increased rates of hazard-producing TCs in the future climate, the probability distribution of the hazard components will also shift towards higher values, with the shift to be most significant for surge (with SLR) hazard, followed by rainfall hazard (Fig. S14).

Besides making weak TCs become hazard-producing, SLR also increases hazard duration (Figure 5). Compared to the projection without considering SLR, the projection with consideration of SLR shows a drastic increase of the average hazard duration. For example, in Texas, the average duration increases from 1.18 days to 1.32 days without considering SLR and 5.93 days considering SLR. This increase in hazard duration caused by the prolonged duration of elevated sea level indicates that TCs at stages of being not very intense or far away from the coast can still produce water levels high enough to be considered hazardous under SLR.

Previous research[29,30] has argued that the change of storm surge caused by storm climatology change may be comparable to, if not dominant over, the effect of SLR, which seems contradictory to the findings of this study. However, previous research focused on the extreme maximum water levels, such as 100-year events. Here we define lower hazard thresholds (i.e., 95-th percentile) that are not extreme but can still cause noticeable impacts. The differences between the findings of this study and previous research imply that SLR is more capable of changing ordinary TC surge events from non-hazard-producing to hazard-producing than of increasing the chances of the most extreme surge events.

“Grey Swan” Sequential Hazard-Producing Storms

In previous sections we examined the events of two “not so extreme” events sequentially impacting the same location, as they may cause enhanced damage. However, if two “Grey Swan” events [31] sequentially impact the United States, dispatching the limited rescue resources to the affected areas may be difficult (e.g., in 2017 for Hurricanes Harvey, Irma, and Maria)[31]. As an example, we investigate the chance of a Katrina-like storm (causing water level >8m) and a Harvey-like storm (causing total rainfall >1000mm) impacting the U.S. coastline sequentially (e.g., impact interval <15 days). Such sequential events cannot be found in the large synthetic dataset under the control climate condition (1375 simulation years). However, sequential impacts from “Katrina” and “Harvey” on the U.S. coastline may occur in the future. Figure 6 shows the return period of such events happening sequentially, with an example pair of “Katrina” and “Harvey” identified in the future synthetic storm simulation. The return period of “Katrina”

and “Harvey” impacting the U.S. coastline within 15 days is around 200 years without considering SLR in the future climate and 85 years with consideration of SLR. The result indicates that the United States should be aware of the chances of being hit by sequential extreme events in the future.

Conclusion And Discussion

This study demonstrates that the chances of sequential TC hazards along the U.S. East and Gulf Coast have increased and may continue to increase. The increased chance of sequential TC hazards is largely driven by the increased TC hazard-producing ability, especially for rainfall and surge hazard (considering SLR). Previous studies have projected TC rain rate to increase by 10%-32%[6,27,28,32,33] by the end of the 21st century. This moderate increase of averaged TC rain rate can drive both the increase of coastal rainfall extremes[6,12,34] and the increase of the proportion of storms that become hazard-producing and eventually increase the chance of sequential TCs hazards. Although TC climatology change dominates the extremes of TC surge and compound flood hazard[6], SLR has a stronger impact on the more moderate events. SLR could double the proportion of TCs producing significant surges to around 80% of landfalling TCs. As uncertainties are reported for the SLR projections[35,36], their role in bringing more TCs that are non-hazard-producing under the current sea level to hazard-producing needs to be further investigated.

The findings in this study are inevitably subject to the uncertainties of the observational data and climate downscaling methods. The data quality of observations in earlier decades is always a concern[37] for TC analysis. However, a clear trend of increased probability of sequential hazard-producing TCs from 1979 (the satellite era) could be found for most study locations (Fig. 2), indicating that the possible missing TC observations in early decades[37] would not significantly alter the conclusions of this study. Also, the general increase of TC intensity in the past decades[21] supports the conclusion of increased hazard-producing capability of landfalling TCs, so that the missing observations of hazards due to equipment failures would likely have limited influence on the conclusion. For climate projection, the major concern was that our synthetic TC model projects increased TC frequency[25], which contradicts several previous studies projecting the opposite[14]. However, the influence of increased TC hazard-producing capability is dominant (considering SLR) over or comparable (without considering SLR) to the influence of increased landfall frequency on the increase of sequential TC hazards, indicating that the uncertainties in TC frequency projection do not significantly influence our conclusion.

This study thoroughly investigated compound hazards from TCs by examining the multi-hazard and temporal-spatial compounding of TCs via analyzing historical record and climate projection. The analysis methods used in this study can be useful for other compound hazards including TC-heatwave and flood-heatwave. Directly analyzing historical trends of compounding events can be challenging due to data limitations, while this study demonstrates that probabilistic models that accurately describe the occurrence of individual events and relationship between them can be used to discover historical trends. Physical-statistical downscaling of extreme events, though with uncertainties, provides a powerful tool

for the projection of compound hazards and the understanding of mechanisms of hazard compounding, and such methods could be developed for the projection of other compound hazards.

This research provides the following take-away messages for the general public. First, this research urges the consideration of back-to-back TC impacts in the development of resilience strategies. Second, TC rainfall and SLR have significant influence on sequential TC hazard events; thus the resilience of coastal infrastructure should be upgraded, targeting future extreme rainfall, prolonged surge, and flooding. Finally, “Grey Swan” temporal-spatial compounding of extreme events, even when impacting different locations, will stretch the emergence response systems in unprecedented ways, so better preparation is needed for emergency response.

Methods

Historical Observations

TCs that made landfall in the United States from 1949–2018 were used for historical trend analysis. The information on historical TCs was obtained from the International Best Track Archive for Climate Stewardship (IBTrACS[38]), which provides six-hourly TC locations and intensities. To quantify and examine the change of impacts from historical landfalling TCs, observations of hourly water levels, daily rainfall, and daily maximum wind at 9 locations across the U.S. coastal areas (location shown in Fig S1) were obtained from the Center for Operational Oceanographic Products and Services (CO-OPS) and National Centers for Environmental Information (NCEI). If the tidal gauge sites had no information for rainfall and wind, we found the closest weather stations to the tidal gauge location and used the rainfall and wind observations in these stations to represent the wind and rainfall hazards at the tidal gauge station.

We found that there was more missing data of wind observation from 1949–1979 than in later decades while the missing data for surge and rainfall observations had no significant decadal variations. To eliminate the possibility that the trends were caused by the more frequent missing wind observations in the earlier decades, similar analysis was conducted for only surge and rainfall hazards, and the same conclusion was reached. The fact that using only surge and rainfall hazards can obtain a similar conclusion as using the triple hazards does not imply that the wind hazard is not important; rather, it implies that the three hazards are physically correlated.

Synthetic TCs

Synthetic TCs generated with a statistical-deterministic TC model[15,25] were used to study the change of sequential hazard-producing TCs in the United States. The synthetic storms used in this study are the same as in ref[6]. The storms were generated under the environment of six CMIP6 climate models (CanESM5, CNRM-CM6-1, GFDL-CM-4, EC-Earth3, IP-SL-CM6A-LR, and MIROC6) for the control (1984-2005) and Shared Socioeconomic Pathway 5 8.5 scenarios (SSP 5 8.5; 2070-2100); 4400 and 6200 U.S. landfalling storms were generated for each model under each scenario, respectively.

Wind Modeling

The complete wind profile model that merges the inner core and outer radii TC wind profiles (C15[19]) was used to simulate the wind hazard associated with the synthetic TCs. To obtain the surface wind affected by environment winds, a correction was added to the simulated wind profile following ref[39]. The C15 model was also used to prepare the required wind input for the TC rainfall simulation.

Hydrodynamical Modeling

The ADCIRC model was used to simulate the storm tides produced by the synthetic TCs. The unstructured computational mesh developed by ref[40], which has a spatial coverage of the entire North Atlantic basin, is used in this study. Eight tidal constituents[41] are applied as boundary conditions at the ocean boundary of the mesh. The wind and pressure fields associated with synthetic TCs are needed for the storm tide simulations and were obtained using physics-based parametric models[42]. This wind model was used in ref[6] to drive surge simulation as it is simpler and has similar performance to the C15 wind model. Further details regarding ADCIRC model and simulation setups can be found in ref[40] .

Rainfall Modeling

The physics-based TC rainfall model (TCR[12]) was used to simulate rainfall associated with the synthetic TCs. Detailed formulation on the TCR can be found in ref (18). The simulation setup of the model followed ref[43], and the environmental field needed for the TCR simulation was obtained following ref[12]. The C15 model was used to drive the TCR rainfall simulation following ref[6] .

Sea Level Rise (SLR) Projection

Localized probabilistic SLR projection[20] under the RCP 8.5 emission scenario was incorporated in this analysis. The projection of SLR[20] was developed for tidal gauge locations; for each point along the coastline, we selected the nearest tide gauge to represent the projected change of SLR in the future. We followed ref[20] to generate multiple SLR values from 2070 to 2100 and randomly drew TC events in each year to combine them with the random SLR value in the corresponding year.

Joint Hazard Analysis

Statistical analysis on the triple of the modeled maximum storm maximum water level (L), maximum daily rainfall (R), and maximum wind speed (W) across each coastal segment of Texas, Louisiana, Mississippi-Alabama, West Florida, East Florida, Georgia, South Carolina, and North Carolina[11] were performed. The marginal distributions of rainfall, surge, and wind were fitted by generalized Pareto distributions (GPDs) to characterize the long tails that corresponding to the extreme events[6,29]. The GPDs were fitted at each coastal segment, and the threshold was set by minimizing the mean squared error between empirical quantiles and the theoretical quantiles[5]. There was no parametric probabilistic

distribution that described the trivariate GPD distributions, so nested Gumbel Copulas[44] were used to represent the dependent structure of the three individual hazards. Gumbel Copulas are used here because previous studies[6,7,45] show that each pair of hazards (surge-rainfall, surge-wind, and wind-rainfall) are correlated especially at tails, and Gumbel Copulas are often used to quantify the tail-dependent structure[46].

After fitting the marginal and joint distributions of the triple of TC hazard, we calculated the probability of three hazards jointly exceeding respective thresholds (joint exceedance probability, or JEP) and the probability of at least one of the three hazards exceeding the respective threshold (at least one exceedance probability, OEP). The thresholds L_T, R_T, and W_T are the marginal return levels of surge, rainfall, and wind hazard with a return period of T years in the control simulation. Thus, JEP and OEP are mathematically defined as:

$$JEP\left(T\right)=\mathbb{P}\left(L>L_T\cap R>R_T\cap W>W_T\right)$$

1

and

$$OEP\left(T\right)=1-\mathbb{P}(L\leq L_T\cap R\leq R_T\cap W\leq W_T)$$

2

To explicitly discuss the effect of SLR, the JEP and OEP under the SSP 5 8.5 scenario were calculated with and without the consideration of SLR. To explore the causation of the change of JEP and OEP, the changes of the exceedance probability of the single hazards (the marginal cumulative density function) were also investigated. The return period (T_{JE}) of the three hazards jointly exceeding respective return level thresholds (under return level T) can be calculated as

$$T_{JE}\left(T\right)=\frac{1}{\lambda\bullet JEP\left(T\right)}$$

3

where λ is the arrival rate of the storms.

Similarly, the return period $\left(T_{OE}\right)$of at least one of the three hazards exceeding the respective threshold can be calculated as

$$T_{OE}\left(T\right)=\frac{1}{\lambda\bullet OEP\left(T\right)}$$

4

Probabilistic Model for Sequential Hazard-Producing TCs

The Poisson-Gaussian model for sequential landfalling TCs developed in ref[11] was extended to capture the storms' hazard-producing ability and hazard durations. The arrival of hazard-producing storms was modeled as a nonstationary Poisson process as

$$\nu\left(t,s\right)=\lambda_{hazard}\left(t\right)S_{hazard}\left(s\right)$$

5

$$S_{hazard}\left(s\right)=\frac{1}{\sigma\sqrt{2\pi}}\mathrm{e}^{-\frac{1}{2}\left(\frac{s-\mu}{\sigma}\right)^{2}}$$

6

where $\lambda_{hazard}\left(t\right)$ is the annual frequency of hazard-producing TCs in year t. $S_{hazard}\left(s\right)$, representing the seasonal variation, is the likelihood of a hazard starting to occur on days relative to the likelihood of occurrence during the season. The difference between the Poisson-Gaussian model in this study and ref[11] is that this study uses the annual frequency and seasonality of hazard-producing storms instead of landfalling storms, and the ratio between the annual frequency of hazard-producing storms and landfalling storms can be viewed as a metric of storm hazard-producing ability. The Poisson-Gaussian model was shown to be capable of capturing the relationship between TC landfall climatology and the minimal landfall intervals[11], and larger frequency (λ_{hazard}) and smaller seasonal span (σ) favors sequential hazard-producing events.

We define the MII mathematically as:

$$\mathrm{MII}\left(\mathrm{t}\right)=\min_{i>j}(\max(B_{i}\left(\mathrm{t}\right)-E_{j}\left(\mathrm{t}\right),0\,))$$

7

where B_i(t) is the hazard beginning time of the i-th TC in year t, and $E_{j}\left(\mathrm{t}\right)$ is the hazard end time of the j-th TC in year t; if the impact of two TCs overlap, we set the MII equal to 0. The TCs in a single year were ordered by the starting time of hazards associated with the TCs. For each individual TC, the beginning times of hazards were randomly drawn from the probabilistic model of Eq. (5) and Eq. (6), and the beginning and end times of hazards were connected as:

$$E_{i}\left(\mathrm{t}\right)=B_{i}\left(\mathrm{t}\right)+D_{i}\left(\mathrm{t}\right)$$

8

where $D_{i}\left(\mathrm{t}\right)$ is the total hazard duration of the i-th TC in year t. As the impact duration of TC-related hazards may change in the future, a probability distribution that describes the duration of TC hazard impact at each selected location is needed. The probability distributions of duration in different coastal

locations under different climate scenarios do not share the same parametric probability distribution. Thus, in our analysis and simulation, we applied kernel density estimation to fit the non-parametric probability distribution to the duration. For climate simulation analysis, the explicit simulation of each hazard component was performed before the probabilistic model was fitted with the simulated synthetic events.

Definition of Hazard-Producing TCs and Hazard Duration

There is no universal definition for “hazard-producing” as different infrastructure systems and communities may respond differently to sequential TC events[11]. A statistically reasonable, physically meaningful, and engineeringly applicable definition of “hazard-producing” should be able to both categorize the landfalling storms into “hazard-producing” and “non-hazard-producing” categories and separate the days of impact from a single “hazard-producing” TC into “hazard days” and “non-hazard days” (such as the days when TCs are too weak or too far away from the point of interest to produce hazards).

To do so, specific percentiles of daily maximum water level, total rainfall, and maximum wind speed were used as the thresholds to define “hazard-producing” TCs. In the historical analysis, for each individual point of interest, the daily maximum water level, total rainfall, and maximum wind from every TC that ever approached 250 km from the location were collected. and the percentiles of each hazard component were calculated based on the observation of all TCs impacting this location. For the climate simulation using CMIP6 models and the synthetic storm model, the same method was applied to calculate percentiles for the control simulation (historical period) of each climate model (so the percentiles differ for the climate models).

The specific percentile chosen as the threshold should be both high enough to eliminate nuisance TC-events and low enough to include some “non-extreme” events that are still hazardous. In this main text of this study, the 95th percentile of each hazard was chosen as the threshold, and the days when at least one hazard component exceeds the threshold were defined as “hazard days.” The threshold was spatially varied by using the 95th percentiles specific to each coastal location to account for spatial variation of the “preparedness” or “awareness” of hazards. The storms that cause at least one “hazard day” for a point of interest were defined as “hazard-producing” storms for this location. The selection of the 95th percentile of threshold fulfills the requirements mentioned in the beginning of this paragraph. For example, the mean of the 95th percentile of 6 climate model simulations of daily accumulated TC rainfall (maximum tide level) in the control climate is 98.8 mm (1.4 m) near New Orleans, which is approximately ¼ (1/6) of the total rainfall (maximum tide level) that Hurricane Katrina (2005) produced in this location. Admittedly, the selection of the 95th percentile was ad hoc, so the results of climate simulations of sequential TC-related hazards under other thresholds (90th and 99th percentiles) are shown in the Supplementary Material as a sensitivity test of the results of this study.

Declarations

Data availability

All data generated in this study, including hazards information and sequential TC hazard statistics, are deposited to the NSF DesignSafe-CI and can be freely accessed online (DOI to be provided upon acceptance). Source data are provided with this paper (upon acceptance).

Code availability

The codes for probabilistic historical/future climate sequential TC hazard events simulation and for visualization are deposited to the NSF DesignSafe-CI and can be freely accessed online (DOI to be provided upon acceptance).

Acknowledgement

D.X. and N.L. were supported by National Science Foundation (NSF) grant numbers ICER 1854993 and 2103754 (as part of the Megalopolitan Coastal Transformation Hub), and by the U.S. Army Corps of Engineers (USACE) Flood and Coastal Systems R&D Program through the Oak Ridge Institute for Science and Education (ORISE) Research Participation Program as part of an interagency agreement between the U.S. Department of Defense (DOD) and the U.S. Department of Energy (DOE). ORISE is managed by ORAU under DOE Contract DE-SC0014664. A.G. was supported by a National Defense Science & Engineering Graduate (NDSEG) fellowship from the US DOD. All opinions expressed in his paper are the authors' and do not necessarily reflect the policies and views of NSF USACE, DOD, DOE, or ORAU/ORISE. We thank Dan Chavas (Purdue University) for his constructive suggestions.

Author information

Authors and Affiliations

Department of Civil and Environmental Engineering, Princeton University, Princeton, NJ, USA

Dazhi Xi, Ning Lin & Avantika Gori

Contributions

D.X. and N.L. designed the study, and N.L. supervised the modelling and analysis. D.X. performed the rainfall and wind modeling, statistical analysis, and probabilistic modeling of sequential TC hazard events. A.G. performed the hydrodynamic modelling. All authors contributed to writing and editing the manuscript.

Ethics declarations

Competing interest

The authors declare no competing interests

References

1. Zscheischler, J. *et al.* A typology of compound weather and climate events. Nature Reviews Earth and Environment vol. 1 333–347 (2020).
2. Matthews, T., Wilby, R. L. & Murphy, C. An emerging tropical cyclone–deadly heat compound hazard. Nature Climate Change vol. 9 602–606 (2019).
3. Feng, K., Min, O. & Lin, N. *Hurricane-blackout-heatwave Compound Hazard Risk and Resilience in a Changing Climate*.
4. Mitsova, D., Esnard, A. M., Sapat, A. & Lai, B. S. Socioeconomic vulnerability and electric power restoration timelines in Florida: the case of Hurricane Irma. Natural Hazards **94**, 689–709 (2018).
5. Gori, A., Lin, N. & Xi, D. Tropical Cyclone Compound Flood Hazard Assessment: From Investigating Drivers to Quantifying Extreme Water Levels. Earth's Future **8**, (2020).
6. Gori, A., Lin, N., Xi, D. & Emanuel, K. Tropical cyclone climatology change greatly exacerbates US extreme rainfall–surge hazard. Nature Climate Change **12**, 171–178 (2022).
7. Pei, B., Pang, W., Testik, F. Y., Ravichandran, N. & Liu, F. Mapping joint hurricane wind and surge hazards for Charleston, South Carolina. Natural Hazards **74**, 375–403 (2014).
8. Mudd, L., Rosowsky, D., Letchford, C. & Lombardo, F. Joint Probabilistic Wind–Rainfall Model for Tropical Cyclone Hazard Characterization. Journal of Structural Engineering **143**, 04016195 (2017).
9. Latto, A. S. & Berg, R. *National Hurricean Center Tropical Cyclone Report Hurricane Nicholas AL142021*. (2022).
10. Shapiro, E., Golembo, M., Griffin, M. & Pereira, I. Nicholas slams Gulf Coast with dangerous flooding. ABC News (2021).
11. Xi, D. & Lin, N. Sequential Landfall of Tropical Cyclones in the United States: From Historical Records to Climate Projections. Geophysical Research Letters **48**, (2021).
12. Emanuel, K. Assessing the present and future probability of Hurricane Harvey's rainfall. Proc Natl Acad Sci U S A **114**, 12681–12684 (2017).
13. Marsooli, R., Lin, N., Emanuel, K. & Feng, K. Climate change exacerbates hurricane flood hazards along US Atlantic and Gulf Coasts in spatially varying patterns. Nature Communications **10**, (2019).
14. Knutson, T. *et al.* Tropical cyclones and climate change assessment part II: Projected response to anthropogenic warming. Bull Am Meteorol Soc **101**, E303–E322 (2020).
15. Emanuel, K. *Climate and Tropical Cyclone Activity: A New Model Downscaling Approach*. (2006).
16. Dietrich, J. C. *et al.* Modeling hurricane waves and storm surge using integrally-coupled, scalable computations. Coastal Engineering **58**, 45–65 (2011).
17. Zhu, L., Quiring, S. M. & Emanuel, K. A. Estimating tropical cyclone precipitation risk in Texas. Geophysical Research Letters **40**, 6225–6230 (2013).
18. Lu, P., Lin, N., Emanuel, K., Chavas, D. & Smith, J. Assessing hurricane rainfall mechanisms using a physics-based model: Hurricanes Isabel (2003) and Irene (2011). *Journal of the Atmospheric*

Sciences **75**, 2337–2358 (2018).

19. Chavas, D. R., Lin, N. & Emanuel, K. A Model for the Complete Radial Structure of the Tropical Cyclone Wind Field. Part I: Comparison with Observed Structure*. Journal of Atmospheric Sciences (2015) doi:10.1175/JAS-D-15.
20. Kopp, R. E. *et al.* Probabilistic 21st and 22nd century sea-level projections at a global network of tide-gauge sites. Earth's Future **2**, 383–406 (2014).
21. Webster, P. J., Holland, G. J., Curry, J. A. & Chang, H. R. Changes in Tropical Ccylone Number, Duration, and Intensity in a Warming Climate. Science (1979) **309**, 1844–1846 (2005).
22. Kossin, J. P. A global slowdown of tropical-cyclone translation speed. Nature **558**, 104–107 (2018).
23. Hall, T. M. & Kossin, J. P. Hurricane stalling along the North American coast and implications for rainfall. npj Climate and Atmospheric Science **2**, (2019).
24. Lee, C. Y., Camargo, S. J., Sobel, A. H. & Tippett, M. K. Statistical-Dynamical downscaling projections of tropical cyclone activity in a warming climate: Two diverging genesis scenarios. Journal of Climate **33**, 4815–4834 (2020).
25. Emanuel, K. Response of global tropical cyclone activity to increasing CO2: Results from downscaling CMIP6 models. Journal of Climate **34**, 57–70 (2021).
26. Jing, R. & Lin, N. An Environment-Dependent Probabilistic Tropical Cyclone Model. Journal of Advances in Modeling Earth Systems **12**, (2020).
27. Knutson, T. R. *et al.* Global projections of intense tropical cyclone activity for the late twenty-first century from dynamical downscaling of CMIP5/RCP4.5 scenarios. Journal of Climate **28**, 7203–7224 (2015).
28. Liu, M., Vecchi, G. A., Smith, J. A. & Knutson, T. R. Causes of large projected increases in hurricane precipitation rates with global warming. npj Climate and Atmospheric Science **2**, (2019).
29. Lin, N., Emanuel, K., Oppenheimer, M. & Vanmarcke, E. Physically based assessment of hurricane surge threat under climate change. Nature Climate Change **2**, 462–467 (2012).
30. Lin, N., Kopp, R. E., Horton, B. P. & Donnelly, J. P. Hurricane Sandy's flood frequency increasing from year 1800 to 2100. Proc Natl Acad Sci U S A **113**, 12071–12075 (2016).
31. Eric Levenson. 3 storms, 3 responses: Comparing Harvey, Irma and Maria. *CNN* (2017).
32. Knutson, T. R. *et al.* Dynamical downscaling projections of twenty-first-century atlantic hurricane activity: CMIP3 and CMIP5 model-based scenarios. Journal of Climate **26**, 6591–6617 (2013).
33. Wright, D. B., Knutson, T. R. & Smith, J. A. Regional climate model projections of rainfall from U.S. landfalling tropical cyclones. Climate Dynamics **45**, 3365–3379 (2015).
34. Zhu, L., Emanuel, K. & Quiring, S. M. Elevated risk of tropical cyclone precipitation and pluvial flood in Houston under global warming. Environmental Research Letters **16**, (2021).
35. Kopp, R. E. *et al.* Usable Science for Managing the Risks of Sea-Level Rise. Earth's Future **7**, 1235–1269 (2019).

36. Kopp, R. E. *et al.* Evolving Understanding of Antarctic Ice-Sheet Physics and Ambiguity in Probabilistic Sea-Level Projections. Earth's Future **5**, 1217–1233 (2017).
37. Moon, I. J., Kim, S. H. & Chan, J. C. L. Climate change and tropical cyclone trend. Nature vol. 570 E3–E5 (2019).
38. Knapp, K. R., Kruk, M. C., Levinson, D. H., Diamond, H. J. & Neumann, C. J. The international best track archive for climate stewardship (IBTrACS). Bull Am Meteorol Soc **91**, 363–376 (2010).
39. Lin, N. & Chavas, D. On hurricane parametric wind and applications in storm surge modeling. Journal of Geophysical Research Atmospheres **117**, (2012).
40. Marsooli, R. & Lin, N. Numerical modeling of historical storm tides and waves and their interactions along the U.S. East and Gulf Coasts. Journal of Geophysical Research: Oceans **123**, 3844–3874 (2018).
41. Egbert, G. D. & Erofeeva, S. Y. *Efficient Inverse Modeling of Barotropic Ocean Tides*. (2002).
42. Emanuel, K. & Rotunno, R. Self-stratification of tropical cyclone outflow. Part I: Implications for storm structure. Journal of the Atmospheric Sciences **68**, 2236–2249 (2011).
43. Xi, D., Lin, N. & Smith, J. Evaluation of a physics-based tropical cyclone rainfall model for risk assessment. Journal of Hydrometeorology **21**, 2197–2218 (2020).
44. Hofert, M. ; & Mächler, M. ETH Library Nested Archimedean Copulas Meet R: The nacopula Package. Journal of Statistical Software **39**, 1–20 (2011).
45. Song, J. Y., Alipour, A., Moftakhari, H. R. & Moradkhani, H. Toward a more effective hurricane hazard communication. Environmental Research Letters **15**, (2020).
46. Ismail, T., Ahmed, K., Alamgir, M., Noor Kakar, M. & Fadzil, A. B. *BIVARIATE FLOOD FREQUENCY ANALYSIS USING GUMBEL COPULA*. Malaysian Journal of Civil Engineering vol. 30 (2018).

Figures

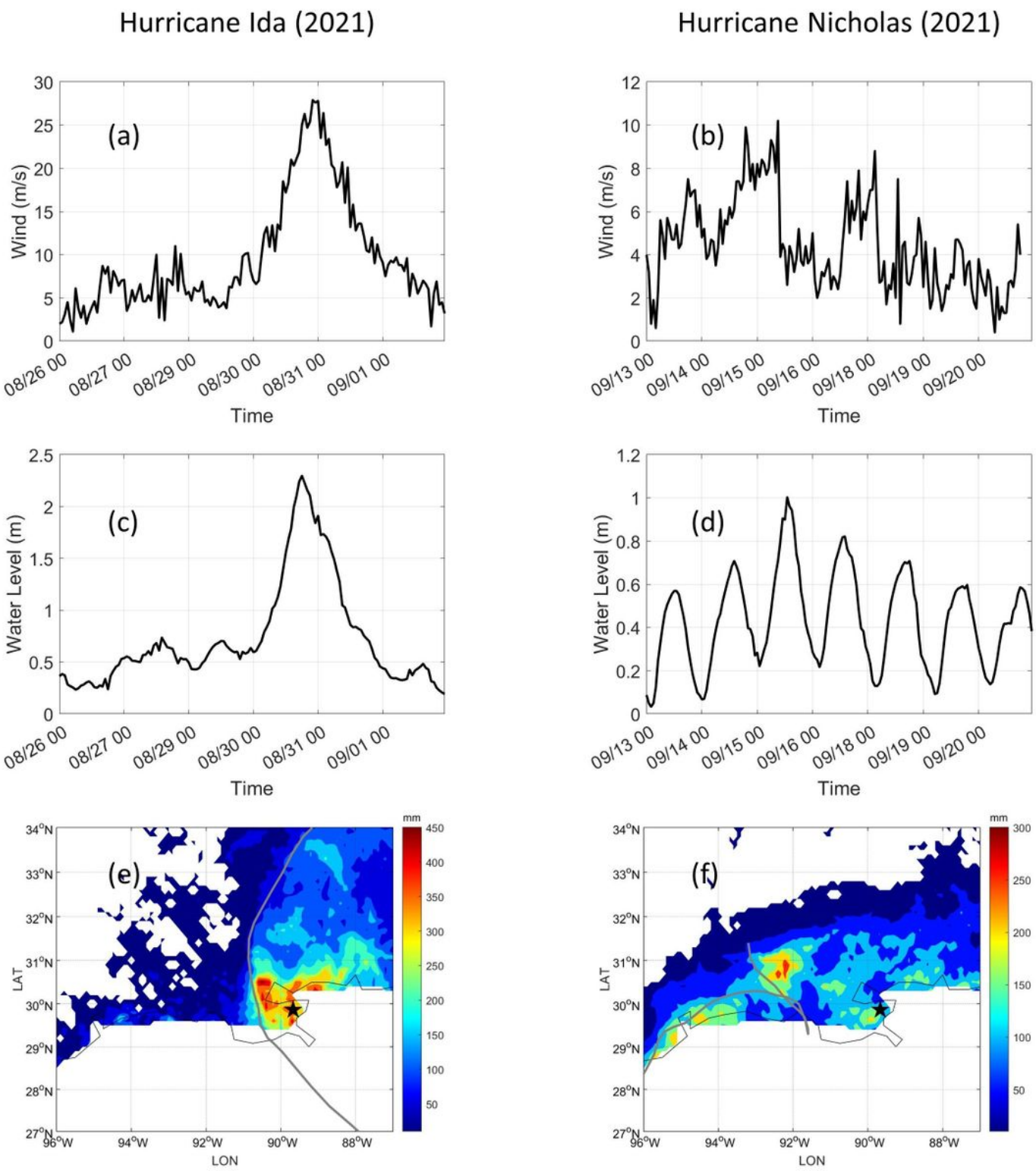

Figure 1

Hazards from Hurricanes Ida (2021) and Nicholas (2021). (a)(b). hourly wind speed at Shell Beach (LA) for Hurricanes Ida and Nicholas, respectively. (c)(d). hourly water level at Shell Beach (LA) for Hurricanes Ida and Nicholas, respectively. (e)(f). total rainfall from Hurricanes Ida and Nicholas, respectively. Location of the tidal gauge at Shell Beach is marked by black pentagram, and storm tracks are shown by grey solid line. The wind and surge observation are obtained from https://tidesandcurrents.noaa.gov/ .

The rainfall observation is obtained from Stage IV radar observation https://data.eol.ucar.edu/dataset/21.093.

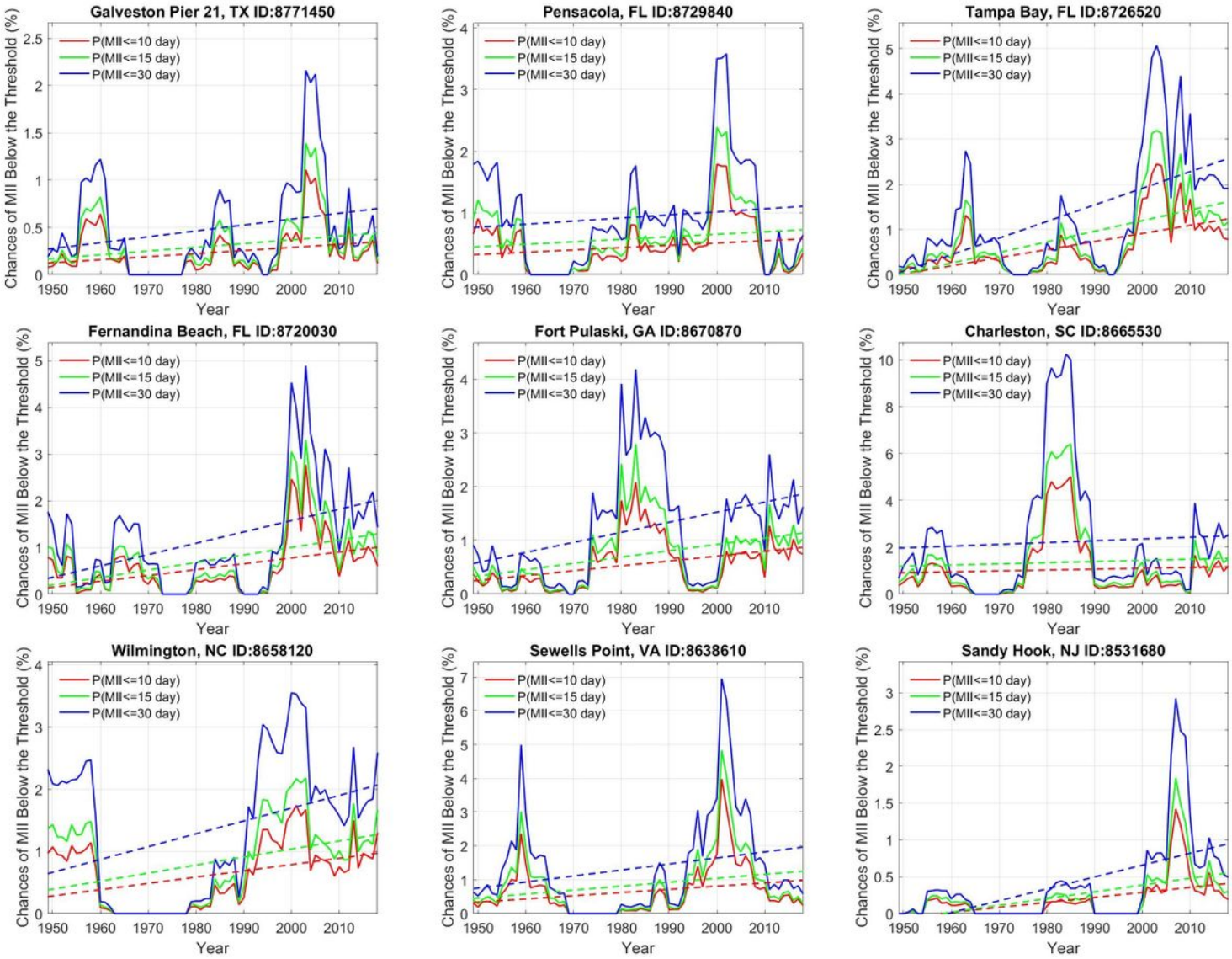

Figure 2

Estimated yearly probability of experiencing sequential hazard-producing TCs, defined as MII smaller than a threshold (10 days, 15 days, and 30 days), in the 9 selected U.S. coastal locations. The dashed lines are fitted linear trends of the probabilities.

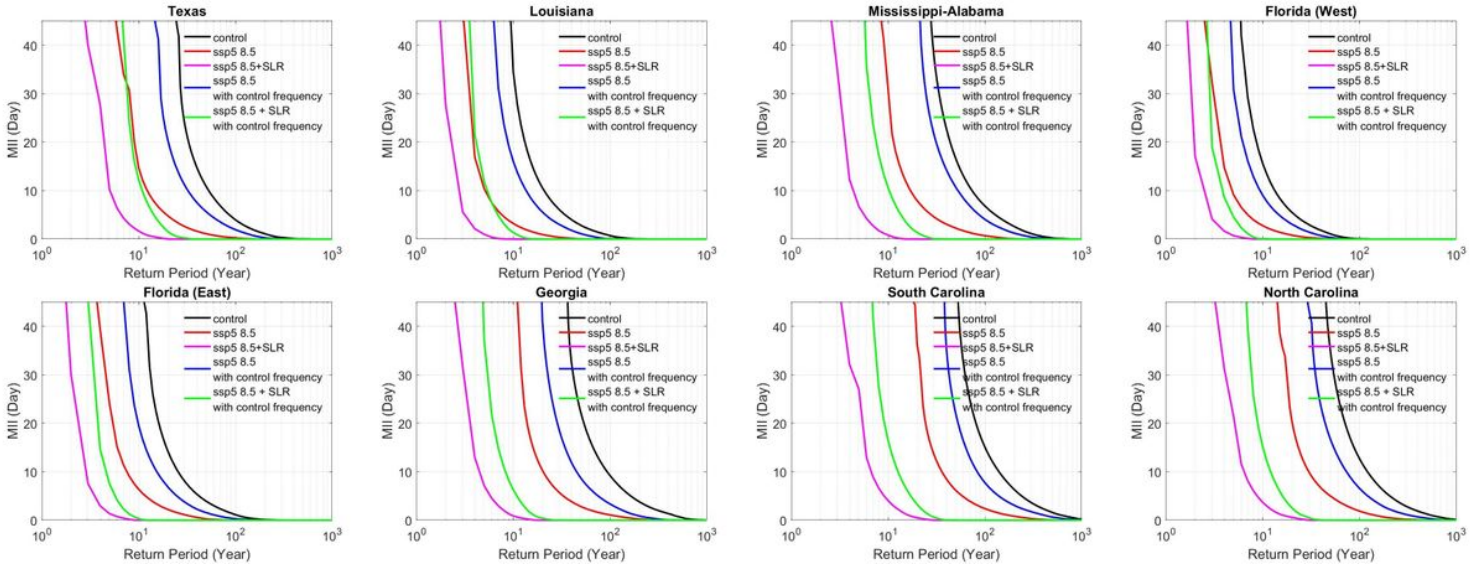

Figure 3

Return period of MII in the climate projection. Black curve: return level of MII in the control period; Red curve: return level of MII in SSP5 8.5 scenario without considering SLR; Pink curve: return level of MII in SSP5 8.5 scenario with consideration of SLR. Blue curve: return level of MII in SSP5 8.5 scenario without considering SLR and storm landfall frequency change. Green curve: return level of MII in SSP5 8.5 scenario considering SLR and without considering storm landfall frequency change. The curves are averaged from six climate models. The results were obtained under the “95-th percentile definition of hazard-producing,” while the results under the “90-th percentile definition” and “99-th percentile definition” are shown in Fig. S6 and Fig. S7, respectively.

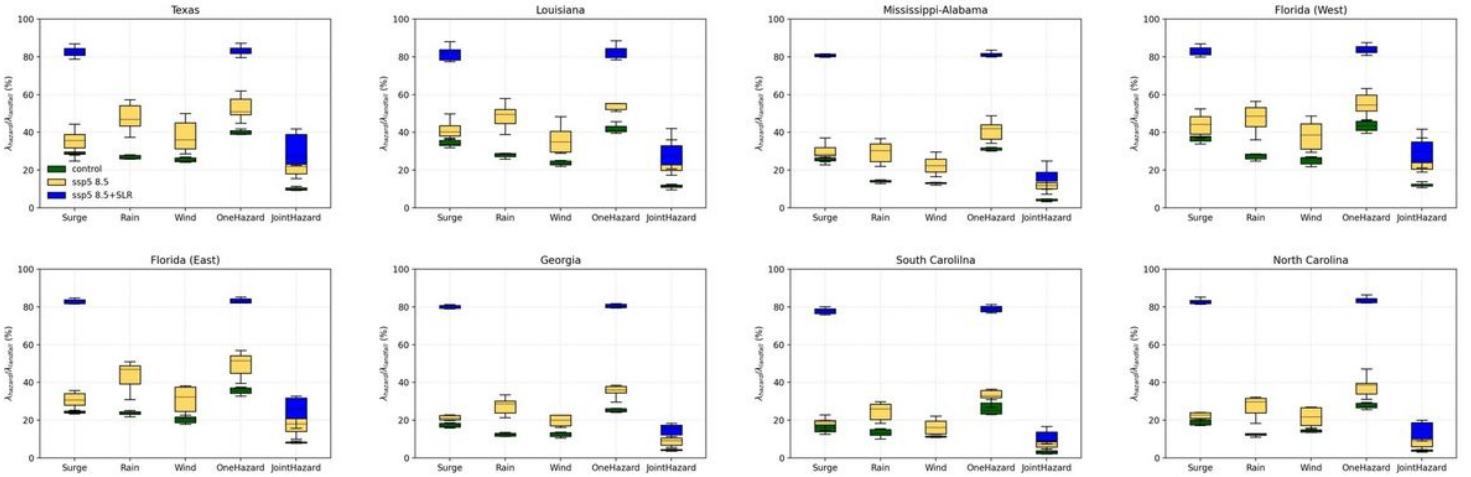

Figure 4

Box plot of the ratio between single hazard-producing, at-least-one hazard-producing, and joint hazard producing TCs and landfalling TCs. The box plot shows the uncertainty among six climate models. Green box: control. Yellow box: SSP5 8.5 without considering SLR. Blue box: SSP5 8.5 with consideration of

SLR. Because in the simulation SLR does not influence rainfall and wind, their ratios in SSP5 8.5+SLR are omitted. The results were obtained under the “95-th percentile definition of hazard-producing” while the results under the “90-th percentile definition” and “99-th percentile definition” are shown in Fig. S8 and Fig. S9, respectively.

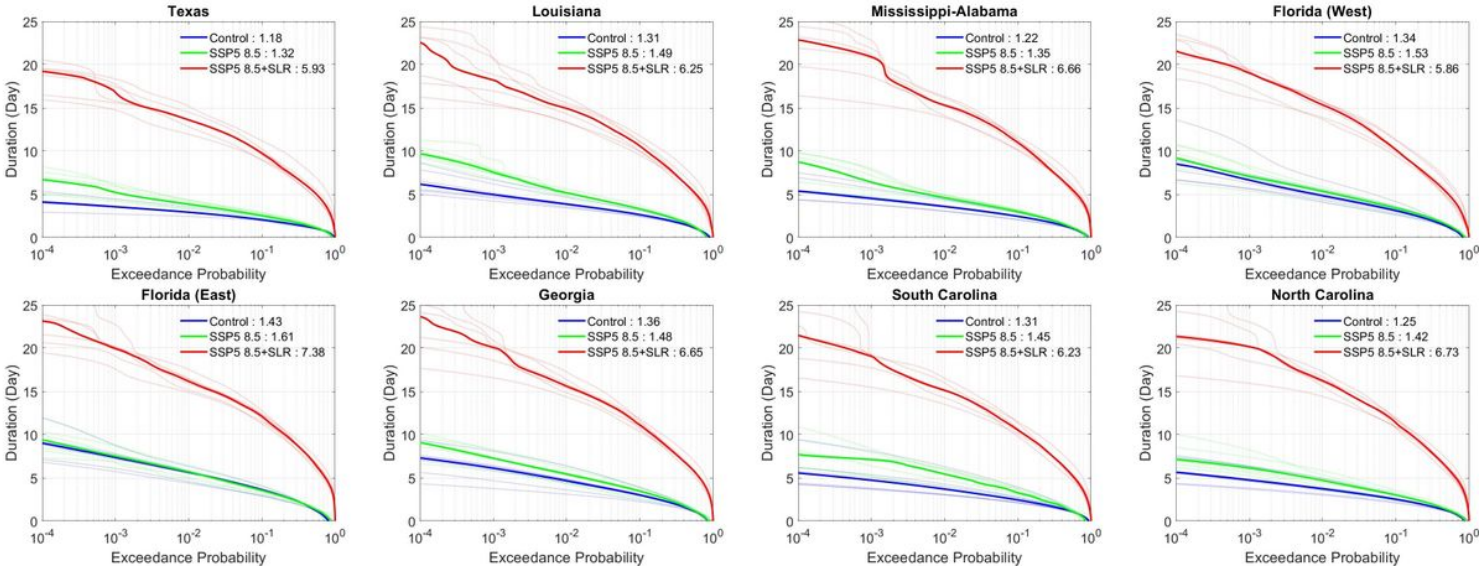

Figure 5

Exceedance probability of hazard duration from TCs. The hazard duration is defined as the total time when at least one hazard component occurs. The exceedance probability is defined as one minus the cumulative probability function. Mean of the hazard duration is presented in the legend.

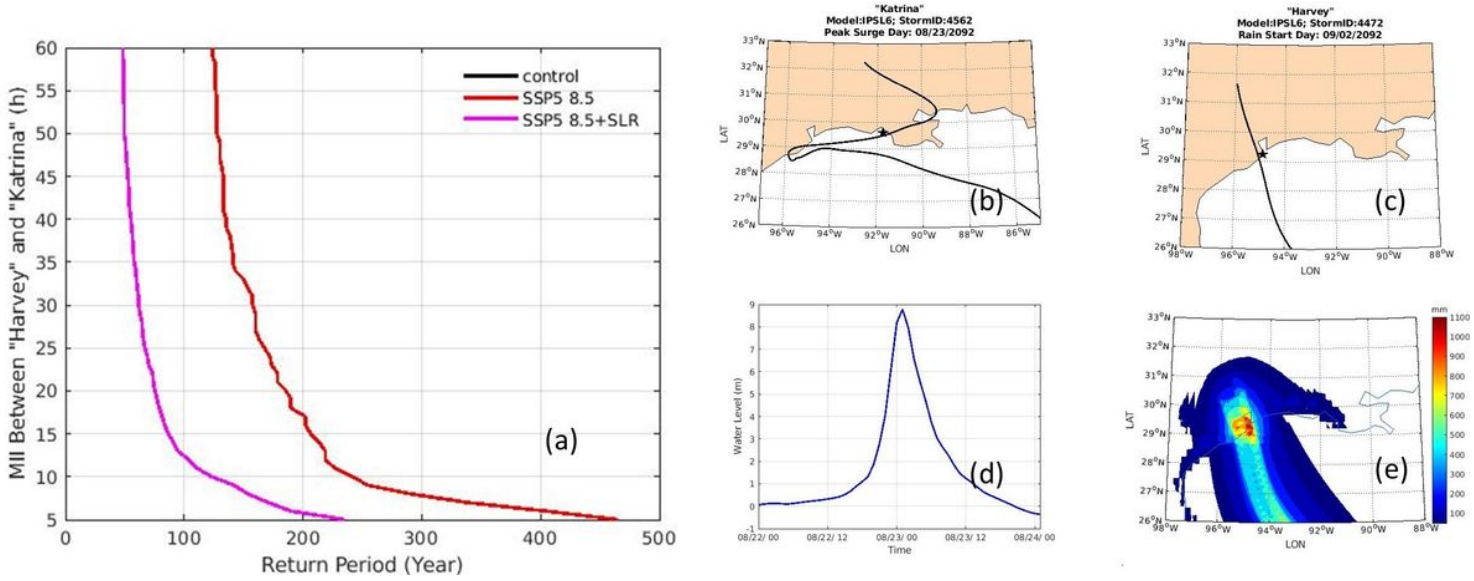

Figure 6

Sequential occurrence of Katrina-like and Harvey-like storms. (a). return period of MII of “Katrina” and “Harvey” impacting the U.S. coastline sequentially. The black curve (return period of the control

simulation) does not exist because no such sequential event can be identified in the control simulation. Here we define a storm to be “Katrina” if it can cause water level higher than 8 m and define a storm to be “Harvey” if it can cause total rainfall greater than 1000 mm in at least one coastal location. (b)(c) selected storm track of “Katrina” and “Harvey,” respectively, from the future synthetic dataset; we chose two storms that have landfall locations similar to historical Katrina (2005) and Harvey (2017). (d) the water level caused by the selected “Katrina”; (e) total rainfall caused by the selected “Harvey,”

Supplementary Files

This is a list of supplementary files associated with this preprint. Click to download.

- supplementaryJune6.pdf